

We thank the reviewer for their thorough evaluation of and constructive feedback on our manuscript. We propose several changes below that we believe address the reviewer's commentary and improve the manuscript. These changes are summarized in this letter, along with specific responses to the reviewer's comments. Below the reviewer's comments our response is shown in blue. Proposed modifications and/or additions to the manuscript are shown in *italics*.

## Reviewer #1 Evaluation

The paper presents a comprehensive discussion of how the neutral wind is and could be considered in height-integrated ionospheric electrodynamics. Rocket and radar measurements are applied to study the actual "effective neutral wind" and evaluate common proxies. The paper is a very interesting contribution to the field of ionospheric electrodynamics and addresses a relevant issue. It can be published with minor revisions. Please see some suggestions below:

- Thank you for the positive feedback!

### 1. Equation 1 and following:

I assume  $\mathbf{b}$  is the unit vector in magnetic field direction, i.e.  $\mathbf{b}=\mathbf{B}/|\mathbf{B}|$ ? Please clarify.

- We will add the following statement just below Equation 1 along with the description of the other variables in Equation 1:

*"The unit vector  $\mathbf{b}$  points in the direction of  $\mathbf{B}$ ."*

### 2. Section 3.3 and Figure 3

The statistics applied here are somewhat unclear to me: What is the statistical meaning of  $Q3+1.5IQR$ ? Also, just roughly estimating for the left box in Figure 3a, IQR seems to be  $\sim 200\text{m/s}$  (with  $Q3\sim 225\text{m/s}$  and  $Q1\sim 25\text{m/s}$ ), but the upper horizontal line ( $Q3+1.5IQR$ ) is at about  $300\text{m/s}$ . This might be a misunderstanding on my part, but in general, I don't see the need for too much statistical analysis on only 15 wind profiles, so just showing the median values and  $Q3$  and  $Q1$  should suffice.

- To the first question, a good way to understand the statistical meaning of  $Q3+1.5 IQR$  is via comparison with a Gaussian distribution. For a Gaussian, values outside of the range defined by  $Q1-1.5IQR$  and  $Q3+1.5IQR$  represent less than 1% of the data. Our understanding is that this rule-of-thumb test for identifying outliers originates with the statistician John Tukey.

To the second question, here the reviewer has identified a mistake in our manuscript (thank you). For all but one box plot, the horizontal lines above and below indicate the maximum and minimum value within each distribution. The exception is in panel b of Figure 3 for  $\mathbf{u}_{\text{proxy}} = \mathbf{u}_{\sigma H, \text{peak}}$ , where the point above the upper horizontal line is an outlier. We will modify the main text as follows in the revised manuscript:

*Each distribution is presented as a vertical box plot, where each box indicates (from top to bottom) the upper quartile  $Q3$ , the median, and lower quartile  $Q1$ . The horizontal lines above and below are respectively given by the largest value not exceeding  $Q3+1.5 IQR$  and the smallest value not below  $Q1-1.5IQR$ , where  $IQR = Q3-Q1$  is the interquartile range. (The range  $Q1-1.5IQR$  to  $Q3+1.5IQR$  is a common rule-of-thumb test for identifying statistical outliers; see, e.g., Dekking et al, 2005.) In Figure 3a these lines simply indicate the minimum and maximum of each distribution, since no values are outside these thresholds.*

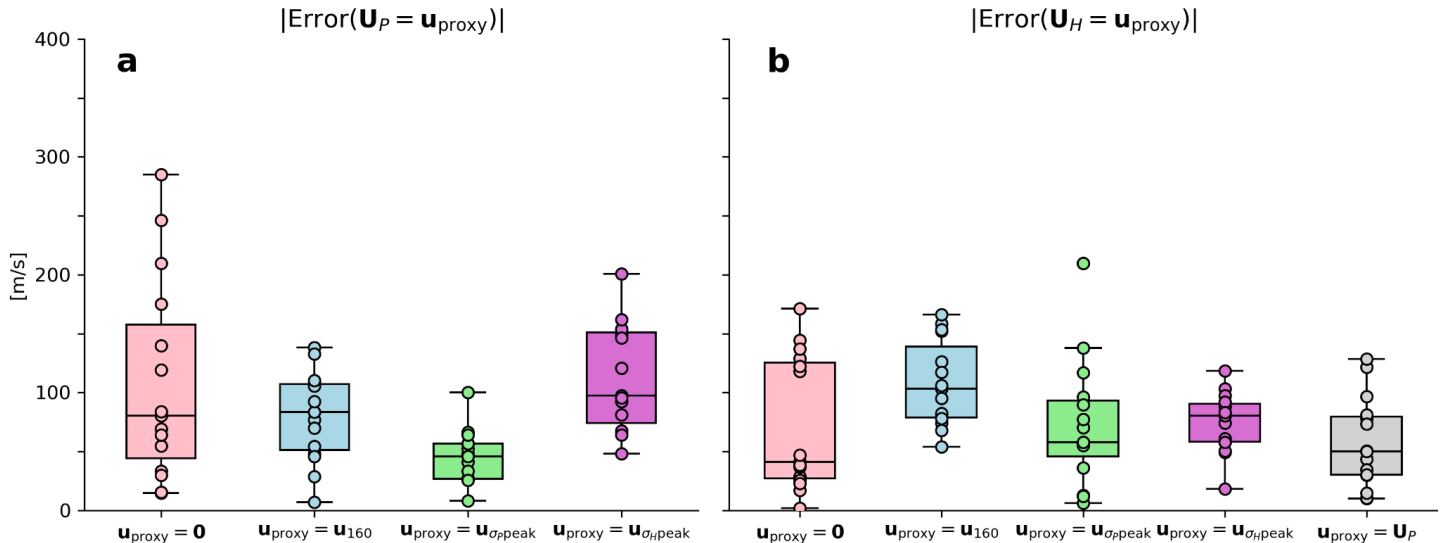
In analogy with Figure 3a, Figure 3b shows the error associated with assuming  $\mathbf{U}_H = \mathbf{u}_{\text{proxy}}$ . One value in the distribution of errors for  $\mathbf{u}_{\text{proxy}} = \mathbf{u}_{\sigma P\text{peak}}$  (shown in green) is identified as an outlier by the rule-of-thumb test mentioned above.

We will also modified the caption for Figure 3 in the revised manuscript as follows:

The horizontal lines above and below each box-and-whisker plot are the minimum and maximum except in panel b for  $\mathbf{u}_{\text{proxy}} = \mathbf{u}_{\sigma P\text{peak}}$ , shown in green, where one value is an outlier (see main text).

With these revisions, we believe the text and figures in the new manuscript will essentially do what the reviewer suggests by showing the median, Q1, Q3, and the minimum and maximum of each distribution except for the one described in the revision. We hope the reviewer will agree that this is a sensible strategy.

- Incidentally, regarding Figure 3 we found a bug in our code that incorrectly calculated the size of the errors associated with assuming the Pedersen-weighted neutral wind  $\mathbf{U}_P$  and the Hall-weighted neutral wind  $\mathbf{U}_H$  are either equal to zero (pink box-and-whisker plot at left in each panel of Figure 3) or  $\mathbf{u}_{160}$  (light blue box-and-whisker plot, second from left). We will replace the old Figure 3 with the following figure:



In the updated figure the correctly calculated errors are smaller for both of these, and  $\mathbf{u}_{160}$  is no longer the obviously worst choice. (In panel b we also added a box-and-whisker plot to assess the performance of  $\mathbf{U}_P$  as a proxy for  $\mathbf{U}_H$ .) We therefore must modify the abstract and several portions of the text in the revised manuscript. We will revise the abstract as follows:

We also find that measurements of the thermospheric wind at altitudes of  $\sim 100\text{--}120$  km are a more accurate estimate of the thermospheric wind terms in expressions of height-integrated, high-latitude electrodynamics than simply assuming the neutral winds are zero in Earth's corotating frame of reference. This points to the possible utility of, for example, Fabry-Perot interferometers that measure 557.7-nm (green-line) emissions around this altitude range.

Also, it seems in Figure 3b that  $u=0$  has a slightly lower median error than the wind at the Pedersen peak. The difference is minor, but contradicts the statement in lines 16 and 17, which is very general in claiming to have found the best proxy (one might come up with other proxies than the four investigated here). Figure 3 suggests

that the Pedersen peak wind could serve as an improved proxy for effective neutral wind compared to the commonly applied  $u=0$  and  $u=u_{160}$ .

- We agree with the reviewer, and acknowledge that there may be other, even better proxies than those we've investigated. We will revise the manuscript so that our claim about the wind at the Pedersen peak is not so absolute and general. We will specifically replace the wording "is the best proxy" in the originally submitted abstract with the revision stated above, which leaves open the possibility of other, even better proxies.

### 3. Lines 223-225

This statement is somewhat confusing. From Lines 111-112, I understood that the Pedersen-weighted neutral wind is the most natural definition of the effective neutral wind, given Equation 11. I do not see the connection to Figure 3, where the Pedersen-weighted neutral wind is used as a baseline to compare different proxies.

- We agree that this statement was confusing. In light of the results contained in the corrected Figure 3 (shown above), we will modify the paragraph on these lines in the revised manuscript as follows:

*Section 3.3 addresses the commonly employed assumption in experimental studies that the winds are zero in Earth's corotating frame of reference, as well as the concept of a two-dimensional "effective neutral wind" pattern introduced by Lu et al. (1995) and employed by both Baker et al. (2004) and Billett et al. (2018). These studies take the effective neutral wind pattern to be the neutral winds at 160-km altitude,  $u_{160}$ , although analysis in Section 2 indicates that a more suitable definition for the effective neutral wind is the Pedersen-weighted neutral wind  $U_P$ , which appears in both the height-integrated Ohm's law (Equation 7) and the lower-bound estimate of Joule heating (Inequality 11).*

*Given the scarcity of simultaneous measurements of the quantities needed to calculate  $U_P$  and  $U_H$  (altitude profiles of conductivities and neutral wind), another motivation for this study is to investigate potential proxies for  $U_P$  and  $U_H$ . Figure 3a explores the accuracy of four proxies for  $U_P$ . Statistically speaking, the best proxy for  $U_P$  is  $u_{P,peak}$ , the neutral wind at the altitude of the peak Pedersen conductivity (located between 115-km and 128-km altitude for the 15 rocket flights presented in Table 1). In contrast, the proxy for  $U_H$  with the lowest median error is the zero vector (pink).*

*Regardless, all proxies perform similarly in the sense that all are associated with errors of order at least several tens of m/s. While this result is subject to the same caveat given above regarding limited sampling, it does suggest that one should be skeptical of "quick fixes" for the neutral wind problem, including ignoring the winds or using wind estimates from higher altitudes such as those estimated via Fabry-Perot interferometers attuned to the 630-nm line (e.g., Shiokawa et al, 2014, and references therein), which tend to cover the F-region ionosphere. On the other hand Fabry-Perot interferometers attuned to 557.7-nm (green-line) emissions, which tend to peak between 100-km and 130-km altitude, could provide neutral wind estimates relevant for analysis of high-latitude IT electrodynamics. The primary caveat with these measurements is that the peak height of green-line emissions can range over ~80- to 180-km altitude via the influence of auroral precipitation (Whiter et al, 2023).*

#### 4. Section 3.4 and associated discussion

It would be interesting to give an estimate of how large the third term of Equation 10 RHS is in comparison to the other two terms, e.g., for a constant electric field or shown as a plot over varying electric field strength. This would allow to assess the inequality in Equation 11 and how good the application of Pedersen-weighted neutral wind as the effective neutral wind is. Also, if I understand Equation 10 correctly, the mix term (second term RHS) also carries some of the difference caused by assuming  $U_P$  as the effective neutral wind? Therefore, why do you focus solely on the exclusively wind-dependent term?

- We chose to focus exclusively on the wind-dependent term since getting an accurate estimate of the electric field for each flight involves significant additional analysis, and would be experimentally demanding, as we have stated at the close of the manuscript. We agree that it would nevertheless be worthwhile and valuable to understand how the third term in Equation 10 compares to the other terms.

To examine the total Joule heating and the role of the neutral wind we propose to add another figure (proposed Figure 5, shown below).

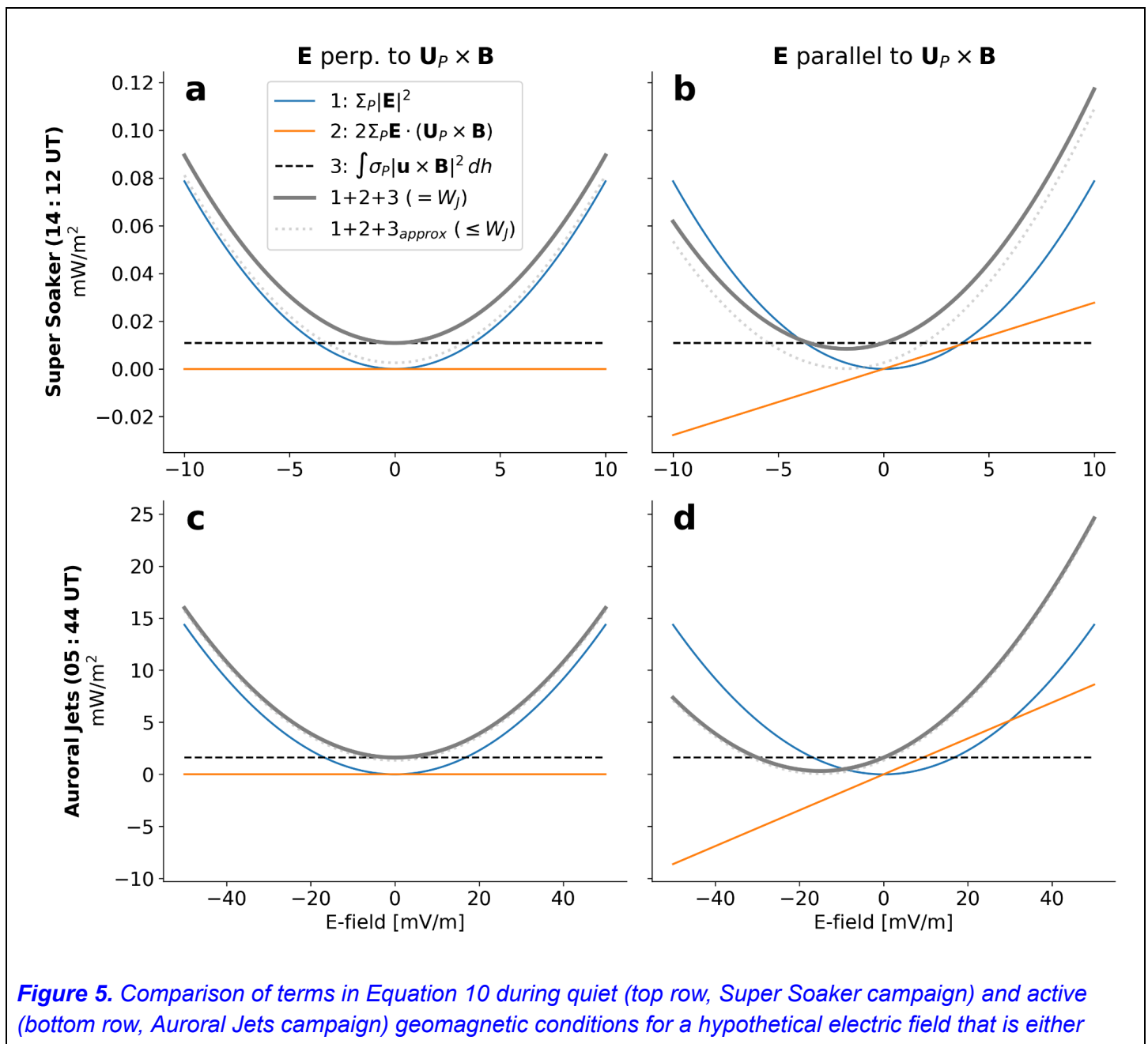


**Figure 5.** Comparison of terms in Equation 10 during quiet (top row, Super Soaker campaign) and active (bottom row, Auroral Jets campaign) geomagnetic conditions for a hypothetical electric field that is either

perpendicular or parallel to  $\mathbf{U}_p \times \mathbf{B}$  (left and right columns, respectively). The blue, orange, and dashed black lines respectively correspond to the first, second, and third terms in Equation 10. The thick, gray line shows the sum of all three terms, and the dotted gray line shows the sum when the third term  $(\int \sigma_p |\mathbf{u}_n \times \mathbf{B}|^2 dh)$  is replaced with the approximation  $\sum_p |\mathbf{U}_p \times \mathbf{B}|^2$ . Note that the range of both Joule heating values and electric field values in the bottom row is larger than in the top row.

We also propose to add the following paragraphs in the discussion section of the revised manuscript:

To further illustrate how the neutral wind affects height-integrated Joule heating, each panel in Figure 5 plots the three terms in Equation 10 as a function of a hypothetical electric field, assuming the electric field is either perpendicular or parallel to  $\mathbf{U}_p \times \mathbf{B}$  (left and right columns, respectively). The values for the neutral wind and Pedersen conductance are taken from the Super Soaker and Auroral Jets campaigns, corresponding respectively to quiet (top row) and active (bottom row) geomagnetic conditions. The total Joule heating (thick gray line) is also plotted in each panel, along with the approximate total Joule heating (dotted gray line) given by replacing the third term  $(\int \sigma_p |\mathbf{u}_n \times \mathbf{B}|^2 dh)$  with the approximation  $\sum_p |\mathbf{U}_p \times \mathbf{B}|^2$ , as in Inequality 11. Electric field values in the top row vary from -10 to 10 mV/m, and from -50 to 50 mV/m in the lower row, corresponding to typical ranges during geomagnetically quiet and active periods (e.g., Walach et al, 2021).

When the electric field is perpendicular to  $\mathbf{U}_p \times \mathbf{B}$  (Figures 5a and 5c), the second term (orange line) is zero by definition. In this case, the total Joule heating  $W_J = \sum_p |\mathbf{E}|^2 + \int \sigma_p |\mathbf{u}_n \times \mathbf{B}|^2 dh$ . The contribution of the neutral winds is to shift the parabola representing Joule heating upward. That is, the neutral winds make a constant and non-negative contribution to the overall Joule heating. The difference between the true total Joule heating and the approximate total Joule heating, dictated by Inequality 11, can be seen by comparing the thick gray line and dotted gray line that respectively represent them.

When the electric field is parallel to  $\mathbf{U}_p \times \mathbf{B}$  (Figures 5b and 5d) the situation is more complicated, since the second term offsets total Joule heating via a linear dependence on the electric field. The two cases shown in these panels illustrate that the vertex, or minimum, is shifted horizontally such that it is located at  $\mathbf{E} = -\mathbf{U}_p \times \mathbf{B}$ . The minimum Joule heating value would be zero if the third term  $(\int \sigma_p |\mathbf{u}_n \times \mathbf{B}|^2 dh)$  were equal to the approximation  $\sum_p |\mathbf{U}_p \times \mathbf{B}|^2$ . It is precisely the difference between the true term and its approximation that causes true Joule heating (thick gray line) to be everywhere greater than zero, in agreement with Inequality 11. When the third term is replaced by the approximation  $\sum_p |\mathbf{U}_p \times \mathbf{B}|^2$ , the minimum of the approximate total Joule heating (dotted gray lines) is zero as expected.

Two additional general conclusions can be drawn from Figure 5: (1) During quiet geomagnetic conditions (top row), the neutral wind influences total Joule heating via both its orientation with respect to the convection electric field (second term, horizontal shifting of the parabola) and its magnitude (third term, vertical shifting). (2) During active conditions (bottom row), the magnitude of the neutral wind is likely less important, with its primary influence being to reduce or enhance the the total Joule heating. This can most easily be seen in Figure 5 as the difference between the parabola that defines the total Joule heating (thick gray line) and the parabola that defines the first term (blue line).

Some estimate of how this affects the Joule heating estimate quantitatively would be appreciated, and I'd suggest stating this in the abstract instead of the sentence in lines 14-17, which seems a bit vague.

- We agree that the lines the referee has pointed to were somewhat vague. In the revised manuscript we will replace them with the following lines, which refer to the new Figure 5 and text describing it in the revised discussion:

*We demonstrate how during geomagnetically quiet periods both the magnitude and direction of the neutral wind may influence total Joule heating, while during active periods the neutral wind influences total Joule heating primarily via its orientation relative to the plasma convection.*